JOURNAL OF APPLIED ELECTROCHEMISTRY 25 (1995) 166–172

Zinc oxoacidity properties in molten LiCl–KCl eutectic at 450° C

H. ROUAULT-ROGEZ, J. BOUTEILLON*, J.-C. POIGNET

Centre de Recherche en Electrochimie Minérale et Génie des Procédés, ENSEEG, BP.75, 38402 St Martin d'Heres, France

Received 6 January 1994; revised 10 June 1994

The solubility of zinc oxide was studied in molten LiCl–KCl eutectic at 450° C. For that purpose, a yttria-stabilized zirconia electrode was employed as a pO^{2-} indicator. The most common calibration methods were reexamined, and it was shown that the 'weighed additions' method failed. The ZnO solubility product was determined.

1. Introduction

From an economic point of view, electrometallurgical processes in molten chlorides are regarded with increasing interest. However, owing to the hygroscopic properties of such media, oxoacidity reactions, i.e. reactions involving exchange of the oxide ion O^{2-} must be well known. For example, during molten salt electrolysis, precipitation of insoluble oxides must be avoided because this reduces current efficiency.

To establish an electrolysis process for pure liquid zinc production from electroreduction of Zn(II) ions in molten LiCl–KCl eutectic at 450° C, we studied the oxoacidity properties of Zn in this solvent. Work on this element at the same temperature has recently been performed but in other molten salt baths: the value of solubility product of the insoluble ZnO oxide has been thus obtained in LiCl–KCl eutectic 5 mol% $ZnCl_2$ [1] and in $ZnCl_2$–2NaCl [2].

Such an investigation requires an O^{2-} activity sensor. Owing to its conductive properties at high temperature, a membrane made of yttria-stabilized zirconia electrode is usually employed in molten chloride systems [3–10].

In the present paper we have first undertaken a reexamination of the behaviour of such an indicator electrode in molten LiCl–KCl eutectic at 450° C. The solubility product of ZnO oxide under the same experimental conditions has then been determined.

2. Yttria-stabilized zirconia electrode

2.1. *Description of the electrode*

The indicator electrode consists of a closed-end tube (5 mm external diameter, 1 mm thickness and 260 mm length) made of yttria-stabilized zirconia (Degussa). It was filled with LiCl–KCl eutectic containing known concentrations of oxide and silver ions (3×10^{-2} and 0.75 mol kg^{-1}, respectively, [10]), which were fixed by adding weighed amounts of Ag_2O and AgCl (quality R. P. Prolabo). A silver wire dipped in this melt formed the inner reference Ag/Ag^+. The measurement of the potential difference between the internal reference electrode and a second reference electrode dipped in the studied electrolyte allows the relationship

$$pO^{2-} = -\log x_{O^{2-}} \quad (1)$$

to be attained, where $x_{O^{2-}}$ is the mole fraction of oxide ions in the electrolyte. The potential of the stabilized zirconia membrane electrode is related to the O^{2-} activity of the external solution by the Nernst relation:

$$E = E^0 + \frac{2.3RT}{2F} pO^{2-} \quad (2)$$

where the value of the term $2.3\,RT/2F$ at 450° C is 0.072 V per decade.

The constant term E^0 depends on both the physical and chemical characteristics of the membrane. Therefore, every zirconia electrode has to be calibrated using a molten solution with known O^{2-} concentration.

2.2. *Principles of some commonly used calibration methods*

The mole fraction of oxide ions can be fixed using well-known chemical equilibria. The most widely employed ones are based on oxoacido-basic buffer systems or on the partial or total dissociation of oxobasic species, as described in the following:

HCl/H_2O 'buffer system'

$$2HCl(g) + O^{2-} \Longleftrightarrow H_2O(g) + 2Cl^- \quad (3)$$

Taking the activity of Cl^- as unity and setting the activities of HCl and H_2O gases equal to their partial pressures (in bar), Lisy and Combes [6] have determined pK_{HCl/H_2O} in molten LiCl–KCl eutectic:

$$pK_{HCl/H_2O} = -2.29 + 10\,030/T \quad (4)$$

* University Joseph Fourier, Grenoble.

0021-891X

Then, at 450° C, the value of the pO^{2-} is given by the relation

$$pO^{2-} = 11.58 + \log\left(\frac{P_{HCl}^2}{P_{H_2O}}\right) \quad (5)$$

CO_3^{2-}/CO_2 'system'

$$CO_3^{2-} \Longleftrightarrow CO_2(g) + O^{2-} \quad (6)$$

The corresponding equilibrium constant

$$K_D = P_{CO_2}\left(\frac{x_{O^{2-}}}{x_{CO_3^{2-}}}\right) \quad (7)$$

is equal to 7.1×10^{-3} at 450° C in LiCl–KCl eutectic [10].

One calibration method is based on the first buffer system, but two calibration methods can be derived using the last system. If the pressure of CO_2 is fixed, the system behaves as a buffer. From Equation 7, pO^{2-} is given by

$$pO^{2-} = 2.15 - \log(x_{CO_3^{2-}}^{add} + x_{CO_3^{2-}}^{0}) + \log P_{CO_2} \quad (8)$$

where $x_{CO_3^{2-}}^{add}$ represents the concentration of carbonate added to the solution and $x_{CO_3^{2-}}^{0}$ the initial CO_3^{2-} concentration before any carbonate addition.

If CO_2 is removed, the carbonate anions can be assumed to be completely dissociated,

$$pO^{2-} = -\log(x_{CO_3^{2-}}^{add} + x_{O^{2-}}^{0}) \quad (9)$$

where $x_{O^{2-}}^{0}$ is the initial oxide mole fraction in the solution. The most widely used calibration method, known as the 'weighed additions' method, is based on the last relationship.

To compare the three common procedures based on the two chemical systems, calibration of a given zirconia electrode has been successively performed.

2.3. *Experimental techniques*

The melt was contained in a 650 ml silica crucible placed in a Pyrex cell described in detail elsewhere [11]. To control the composition of the inner atmosphere the cell was hermetically sealed. The upper cover contained passages in order to introduce electrodes, controlling thermocouple and tubes for gas flow. The sodium carbonate was added through an impervious lock chamber. The temperature of the molten salt was maintained constant within ±1 K by means of a Hermann Morizt furnace [12]. Taking into account the sensitivity of the zirconia membrane to thermal shock, heating and cooling rates were below 80° C per hour.

The LiCl–KCl eutectic melt was prepared according to a well established procedure [10, 11, 13, 14]. It was fused under a dry argon atmosphere, containing less than 0.4 p.p.m. H_2O and 0.1 p.p.m. O_2 before entering the galvanic cell [11].

Gaseous mixtures of HCl and H_2O were obtained by passing pure dry argon gas through a thermostatted aqueous solution of hydrogen chloride. The partial pressures of HCl and H_2O were fixed by both the temperature and the concentration of the aqueous hydrochloric acid solution (supplied by Prolabo). Their values are reported in 'International Critical Tables' [15].

To use the CO_3^{2-}/CO_2 buffer system, the carbon dioxide pressure was maintained at atmospheric. The gas (an Airgas product) was predried and simply bubbled through the molten salt. To use the 'weighed additions' method, a null CO_2 partial pressure was maintained by using an intense argon flow over the bath surface through a cranked tube. Carbonate ions were introduced into the melt using weighed amounts of sodium carbonate (Prolabo) which were predried before addition.

The potential measurement was made with respect to an outer reference electrode which consisted of a silver wire (0.5 mm diam.) dipped in a LiCl–KCl solution of silver chloride (0.75 mol kg^{-1}), contained in a closed-end Pyrex glass tube [16]. The e.m.f. was measured by means of a high impedance voltmeter (HP multimeter 34401A) and recorded on a HP computer with a G.W. Basic program. It corresponds to the following cell:

$$\underbrace{\mathrm{Ag}\left|\begin{array}{c}\mathrm{LiCl}+\mathrm{KCl}\\ [\mathrm{AgCl}]_x \quad [\mathrm{O}^{2-}]_y\end{array}\right|\mathrm{ZrO_2}\text{–}\mathrm{Y_2O_3}}_{\text{zirconia indicator electrode}} \times \left|\begin{array}{c}\mathrm{LiCl}+\mathrm{KCl}\\ \mathrm{pO}^{2-}\text{to be measured}\end{array}\right| \times \underbrace{\mathrm{Pyrex}\left|\begin{array}{c}\mathrm{AgCl\ in}\\ \mathrm{LiCl}+\mathrm{KCl}\end{array}\right|\mathrm{Ag}}_{\text{outer reference electrode Ag/AgCl}}$$

2.4. *Setting-up of the calibration methods*

For the HCl/H_2O and CO_3^{2-}/CO_2 buffer systems, for each imposed oxide concentration, the electrode potential reached a stable value within ±5 mV after less than 1 h and 5 h, respectively.

For the 'weighed additions' method, the time necessary for the potential to reach a constant value was governed by the kinetics of dissociation of sodium carbonate. The measurement of the potential corresponding to the complete dissociation of carbonate requires an examination of its evolution over a long time, as shown in Fig. 1: the potential decreased rapidly for a few hours. After typically 7 h, the rate of decrease then slowed down (less than 5 mV per hour) and the potential tended towards a constant value within ±5 mV after typically 24 h. This constant value was chosen as corresponding to the total dissociation of the added carbonate ions.

Moreover, whatever the mass of added carbonate, we observed that from this constant value the potential started to increase towards a reproducible value

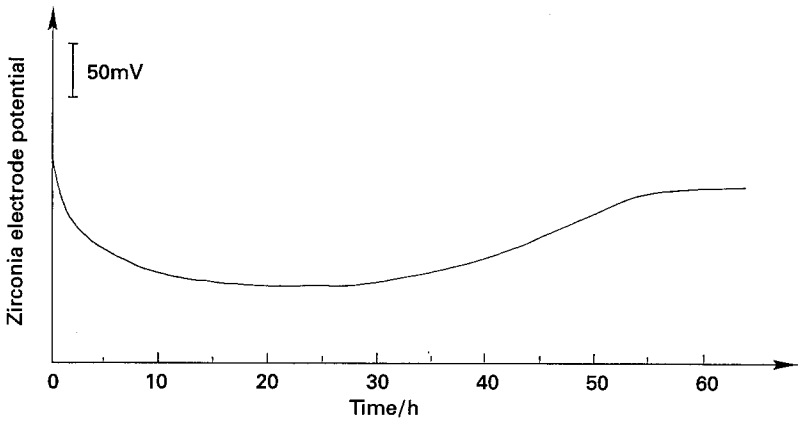

Fig. 1. Typical variation of the zirconia electrode potential when sodium carbonate is introduced into molten LiCl–KCl eutectic under argon atmosphere.

(Fig. 1). This value corresponded to $pO^{2-} = 6$ according to the calibration curve, and was close to the measured value of the zirconia electrode potential detected when 'dry' argon was bubbled through pure molten LiCl–KCl eutectic at 450° C. This limiting value of $pO^{2-} = 6$ was also reached when, from a high potential value imposed by the gaseous mixture of HCl and H_2O, argon was bubbled through the melt. Thus, argon bubbling caused the oxide ions to be removed until equilibrium with the residual water vapour pressure contained in the dry argon flow was established. Water vapour behaved as an oxo-amphoter species, according to the following reactions [3]:

$$2HCl(g) + O^{2-} \Longleftrightarrow H_2O(g) + 2Cl^- \qquad (3)$$

or

$$H_2O(g) + O^{2-} \Longleftrightarrow 2OH^- \qquad (10)$$

With the 'weighed additions' method, it was noticed that the measurement of the potential depended on the argon flow rate when this flow was not sufficiently large. For low flow rates the measured potential value appeared too high and corresponded to an oxide ion concentration lower than expected. This phenomenon may be attributed to an inadequate removal of gaseous CO_2 resulting from carbonate dissociation. In these conditions, total dissociation was not obtained. These results show the difficulties linked to the 'weighed additions' method.

Therefore, the two first methods based on oxoacido-basic buffer systems are fast and efficient, but limited to a narrow pO^{2-} domain, taking into account the values of the equilibrium constants and of the gas partial pressure ranges or minimum, usable sodium carbonate masses. The third method is the most widely used because it is simple and easy from a theoretical and experimental point of view. However, it must be employed carefully because of the influence of the argon flow rate on the CO_2 gas elimination and also because of the difficult choice of a significant value for the potential of the zirconia electrode.

By testing these three methods, and especially that based on the HCl/H_2O buffer system, we also noticed that the response of the zirconia electrode potential to a change in oxide concentration was fast. The long time needed to reach a stable potential, particularly observed with the CO_3^{2-}/CO_2 system, may be attributed to the slow establishment of the dissociation equilibrium, rather than to the electrochemical kinetics of the indicator electrode.

2.5. *Results*

Taking into account the above remarks, we measured values of the zirconia electrode potential with respect to the oxide ion concentration. The results are presented in Table 1 for the HCl/H_2O buffer method, Table 2 for the CO_3^{2-}/CO_2 buffer method and Table 3 for the 'weighed additions' method. In Tables 2 and 3, the pO^{2-} values have been calculated taking into account the correction term $x^0_{CO_3^{2-}}$ corresponding to the presence of CO_3^{2-} resulting from the substitution of the gaseous $Ar + HCl + H_2O$ mixture by CO_2 gas. The potential versus pO^{2-} curve is shown in Fig. 2. The experimental points are well situated on the calibration straight line, the equation of which is

$$E(\text{mV}) = -471 + 62.8\,pO^{2-} \qquad (11)$$

This calibration curve obeys the theoretical Nernstian law (Relation 2).

Table 1. Values of the zirconia electrode potential E with respect to pO^{2-}, corresponding to differing concentrations of aqueous HCl acid solution maintained at 20° C

HCl solution concentration/wt %	P_{HCl}*/mm Hg	P_{H_2O}†/mm Hg	pO^{2-} *(mole fraction scale) Relation 5*	*E*/mV
28	4.9	6.32	9.3	144
32	50.5	3.81	11.5	240
36.6	132.0	2.95	12.5	303

* P_{HCl} partial pressure of HCl from [15].
† P_{H_2O} partial pressure of H_2O from [15].

Table 2. Values of the zirconia electrode potential E with respect to pO^{2-}, corresponding to differing carbonate addition under an atmospheric pressure of CO_2. Before any addition, E was equal to −98 mV in pure argon atmosphere and −49 mV in CO_2. Thus, the value of $x^0_{CO_3^{2-}}$ of 2.16×10^{-5} was deduced

$x^{add}_{CO^{2-}_3}$	pO^{2-} (*mole fraction scale*) *Relation 8*	*E*/mV
1.3×10^{-5}	6.6	−66
5.6×10^{-5}	6.3	−78
2.3×10^{-4}	5.8	−102

Finally, each of the three procedures were consistent with the other two and allowed calibration of the yttria-stabilized zirconia electrode over a large range of pO^{2-} from 2 to 13, and the verification of its Nernstian behaviour in LiCl–KCl eutectic at 450° C [10]. This indicator electrode will be used to determine the solubility product of ZnO in the same experimental conditions.

3. The ZnO solubility product

The ZnO solubility product $K_S(ZnO)$ is defined by the following relation:

$$K_S = x_{Zn(II)} \times x_{O^{2-}} \qquad (12)$$

where $x_{Zn(II)}$ and $x_{O^{2-}}$ represent, respectively, the mole fraction of Zn(II) and O^{2-} species. In fact, $K_S(ZnO)$ is an apparent solubility product, because of the differing possible forms of the Zn(II) species (free Zn^{2+}, zincates, chlorozincates).

3.1. *Solubility product determination*

The solubility product can be determined by two procedures: either $x_{Zn(II)}$ is maintained constant in LiCl–KCl eutectic and the oxide ion concentration corresponding to ZnO precipitation is determined, or inversely $x_{O^{2-}}$ is fixed and the Zn(II) species concentration at the onset of ZnO precipitation is measured. In all cases, $x_{O^{2-}}$ is determined using the zirconia electrode.

The first method has been primarily tested. The Zn(II) species concentration was fixed by dissolution of a weighed quantity of $ZnCl_2$ zinc chloride (Prolabo product) into molten LiCl–KCl eutectic. Oxide ions were introduced into the mixture by addition of weighed amounts of sodium carbonate in an argon atmosphere.

Table 3. Values of the zirconia electrode potential E with respect to pO^{2-}, corresponding to differing amounts of carbonate addition in a dry argon atmosphere. The initial oxide concentration $x^0_{O^{2-}}$ is 2×10^{-5}

$x_{CO_3^{2-}}$	*Gas flow*	pO^{2-} (*mole fraction scale*) *Relation 9*	*E*/mV
2.3×10^{-4}	CO_2*	5.8	−102
	argon	3.6	−238
3.8×10^{-4}	argon	3.4	−277

* Result from the earlier method.

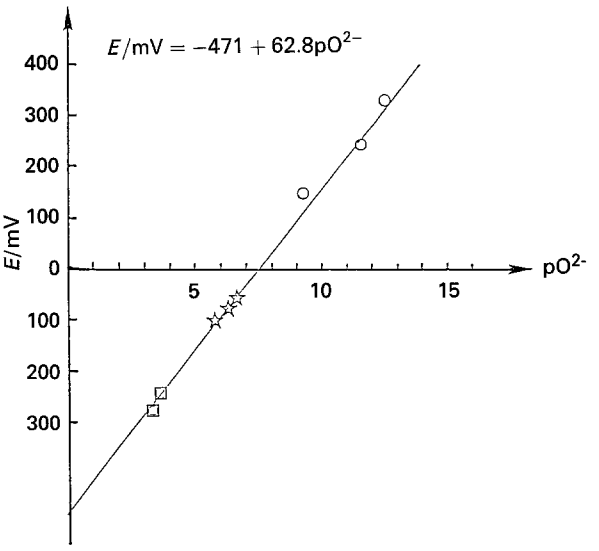

Fig. 2. Calibration curve of yttria-stabilized zirconia electrode. Key: (○) HCl/H_2O buffer system; (☆) CO_3^{2-}/CO_2 buffer system; (□) 'weighed additions' method.

However, no interpretation of the evolution of the zirconia electrode potential (i.e. of the oxide concentration) could be clearly established. Differing weights of added sodium carbonate gave two types of zirconia electrode responses, summarized in Fig. 3. In both cases, whatever the added quantity, the potential (thus the pO^{2-}) decreased as soon as carbonate was introduced, resulting from the CO_3^{2-} decomposition, and finally increased again systematically towards the initial value corresponding to $pO^{2-} = 6$.

When the quantity of carbonate was too low in order to induce ZnO precipitation (curve (a)), the O^{2-} species were removed from the melt because of the establishing equilibrium with oxoacid residual water vapour in argon: no plateau was observed on the curve.

In contrast, when enough sodium carbonate was added, three regions on the experimental curve (noted (b) on Fig. 3) could be distinguished: part I corresponds mainly to the dissociation of carbonate ions. The plateau II may be due to the precipitation of zinc oxide. Along part III, the pO^{2-} decreases as long as the process of carbonate dissociation is operating, and then it increases for the reason mentioned above (Section 2.4). Nevertheless, the measurement of the potential corresponding to the plateau for several additions did not yield reliable results. The plateau II may not result from pure ZnO precipitation, because equilibrium reactions linked to the oxoacido-basicity properties of H_2O interfere. This method failed and appeared unusable. Consequently, the second method was used.

The pO^{2-} of the electrolyte was maintained constant by the CO_3^{2-}/CO_2 buffer system under an atmospheric pressure of carbon dioxide (Relation 8). Zn(II) species were then supplied into the molten solution by zinc anodic oxidation, by the reaction

$$Zn \longrightarrow Zn(II) + 2e^- \qquad (13)$$

The principle of the method is as follows. The

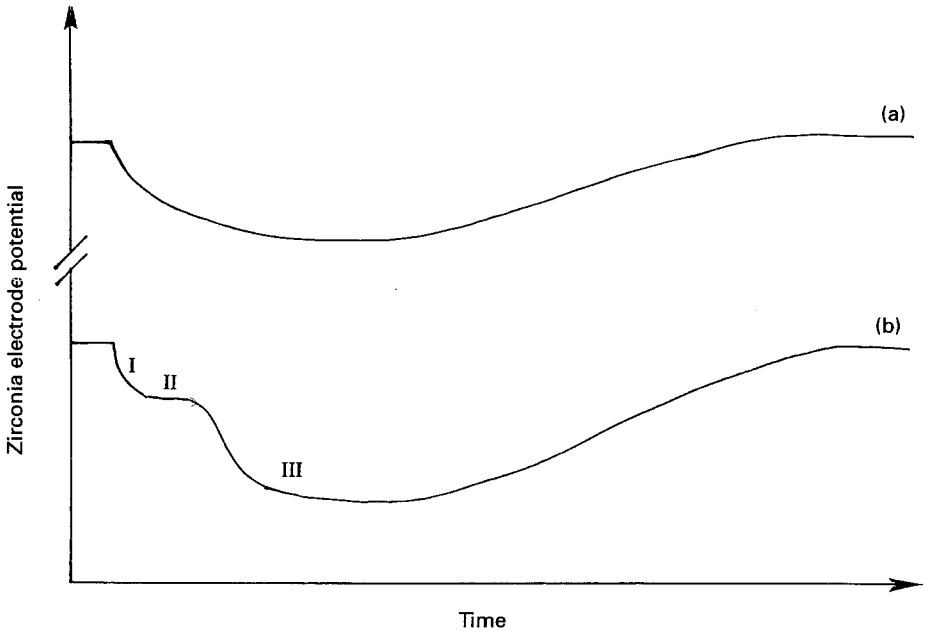

Fig. 3. Typical responses of the zirconia electrode when sodium carbonate is introduced into molten LiCl–KCl eutectic–0.3% $ZnCl_2$ under argon atmosphere, according to a low (a) or a high (b) carbonate mass.

Zn(II) species concentration in the electrolyte was determined from the value of the open circuit potential of a zinc electrode. This potential should first increase according to the Nernst equation,

$$E_{Zn/Zn(II)} = E^0_{Zn/Zn(II)} + \frac{2.3\,RT}{2F} \log x_{Zn(II)} \qquad (14)$$

where $E_{Zn/Zn(II)}$ and $E^0_{Zn/Zn(II)}$ represent the potential and the apparent standard potential of the Zn/Zn(II) couple, respectively.

The zinc electrode potential should remain constant from the onset of zinc oxide precipitation. Thus, from the limiting value of $x_{Zn(II)}$ noted x_p, and from the fixed value of $x_{O^{2-}}$, the magnitude of the solubility product can be calculated from Relation 12.

3.2. *Experimental details*

Two experiments were performed with two fixed values of $pO^{2-} : pO^{2-} = 3$ and $pO^{2-} = 4$.

These experiments were conducted in the same galvanic cell described above (Section 2.3). Its arrangement is presented in Fig. 4. The silica crucible had two compartments in order to prevent the reduction of the Zn(II) species formed by anodic oxidation during electrolysis. The cathodic compartment was the crucible itself containing a zinc chloride solution ($x_{Zn(II)} = 5 \times 10^{-3}$) and the cathode consisted of a tungsten wire (Alfa product with a diameter of 1 mm) immersed in the catholyte. The anodic compartment was constituted by a thin-wall spheric bubble (33 mm diameter) at one end of a Pyrex glass tube (Fig. 5). It contained 6 cm^3 of molten LiCl–KCl eutectic melt with a fixed oxide concentration (supplied by a known weight of sodium carbonate) and about 3 g of pure liquid zinc (Prolabo). A tungsten wire immersed into the liquid zinc pool and sheathed by a Pyrex glass tube formed the zinc electrode which constituted the anode. Its equilibrium potential was measured against a Ag/AgCl reference electrode also placed in the anodic compartment. The zirconia pO^{2-} indicator electrode was immersed in the anolyte. Gaseous CO_2 was bubbled through this solution by a narrow Pyrex glass tube and flowed up to the cathodic compartment.

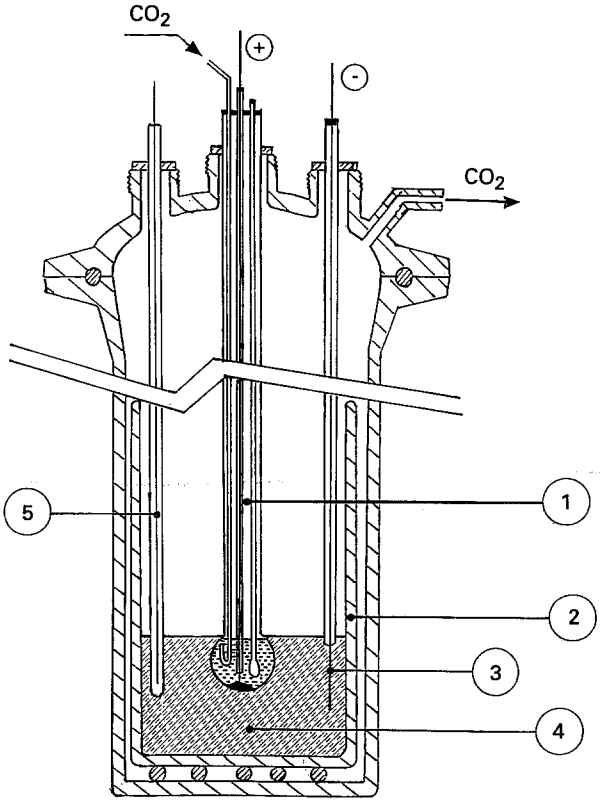

Fig. 4. Electrolysis cell adapted to the study of the zinc oxoacidity properties: (1) anodic compartment; (2) cathodic compartment; (3) cathode; (4) LiCl–KCl eutectic containing 0.5% $ZnCl_2$; (5) controlling thermocouple.

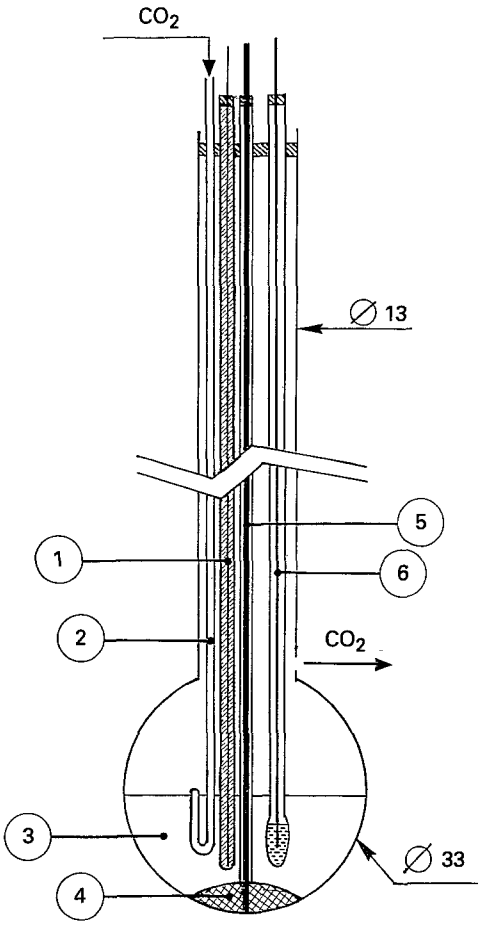

Fig. 5. Anodic compartment for the study of zinc oxoacidity properties: (1) zirconia electrode; (2) Pyrex glass tube for bubbling CO_2 gas; (3) LiCl–KCl eutectic with fixed pO^{2-}; (4) pure liquid zinc pool; (5) tungsten wire protected by Pyrex glass tube; (6) Ag/AgCl reference electrode.

The Zn(II) species concentration in the anolyte was gradually increased coulometrically by a series of electrolyses performed using a CNB Electronic galvanostat. The applied currents ranged from 2 to 10 mA and the duration of each electrolysis was taken correspondingly between 10 and 15 h for the lowest current and only one minute to 3 h for the maximum current. After each anodic oxidation sequence, the equilibrium potential of the zinc electrode was measured while the amount of Zn(II) species supplied by successive electrolysis in the anolyte was calculated on the basis of Faraday's law, assuming that current efficiency was 100%.

3.3. *Experimental results*

The equilibrium potentials of the zinc electrode $E_{Zn/Zn(II)}$ are displayed with respect to the calculated

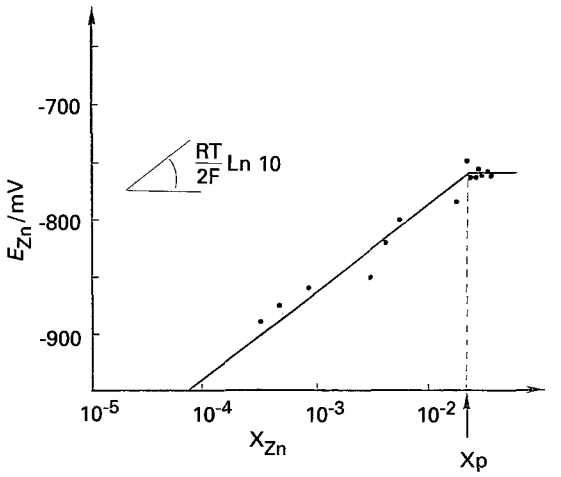

Fig. 6. Variation of equilibrium potential of the zinc anode with respect to the total concentration of Zn(II) species formed by oxidation into the anolyte where pO^{2-} is 4.

total concentration of formed Zn(II) species $x_{Zn(II)}$ on a semi-logarithmic plot. Figure 6 shows the data deduced from the experiment with pO^{2-} equal to 4. As anticipated, the experimental points fit reasonably well a straight line the slope of which is consistent with a two electron exchange at 450° C (Relation 14), and from the detectable value x_p, they then begin to form a plateau. When reaching the plateau, the precipitation of insoluble zinc oxide was visually observed through the cell wall. Formation of insoluble zinc carbonate is not questionable because pO^{2-} remained constant. Indeed, under atmospheric carbon dioxide pressure, precipitation of $ZnCO_3$ should induce an increased oxide ion concentration; this was not observed.

A few erratic potential values were measured. These are attributed to the formation of a superficial oxide layer on the zinc electrode due to a gradient of Zn(II) species concentration. Indeed, moving the electrode or stirring the anolyte induced a potential drop, possibly because the oxide layer was disrupted. The quality of the electrical contact between the tungsten lead and molten lead is not questionable, because tungsten is insoluble in pure liquid zinc and perfectly wetted by this metal [17, 18].

From linear regression analysis of the experimental data, assuming the slope value of the straight line as equal to 72 mV per decade, the magnitude of $E^0_{Zn/Zn(II)}$ against the Ag–AgCl reference was deduced for each test:

$$E^0_{Zn/Zn(II)} = -595 \pm 80\,mV \quad \text{for} \quad pO^{2-} = 3$$

$$E^0_{Zn/Zn(II)} = -630 \pm 50\,mV \quad \text{for} \quad pO^{2-} = 4$$

Table 4. Values of the solubility product K_S of zinc oxide ZnO in molten LiCl–KCl eutectic at 450° C. x_p is the Zn(II) species concentration in the anolyte when ZnO is precipitating, determined from the experimental curve, x_p^{exp}, and from chemical analysis of the anolyte, x_p^{anal}

pO^{2-} (*mole fraction scale*)	x_p^{exp}	K_S^{exp} (*mole fraction scale*)	x_p^{anal}	K_S^{anal} (*mole fraction scale*)
3	$[1 \times 10^{-3}–6.3 \times 10^{-3}]$	$[1 \times 10^{-6}–6.3 \times 10^{-6}]$	1.1×10^{-3}	1.1×10^{-6}
4	3.2×10^{-2}	3.2×10^{-6}	2.4×10^{-2}	2.4×10^{-6}

Table 4 presents the values of the solubility product $K_S(ZnO)$ calculated from the deduced values of x_p^{exp} and from the Zn(II) species concentration, x_p^{anal}, obtained from chemical analysis of the anolyte when ZnO precipitation was observed. The results are consistent.

Finally, the magnitude of the cologarithm of the solubility product of ZnO in LiCl–KCl eutectic at 450° C is $pK_S = 5.6 \pm 0.3$, (correspondingly $K_S(ZnO) = 2.5 \times 10^{-6}$) on the molar fraction scale and $pK_S = 3.1 \pm 0.4$, (correspondingly $K_S(ZnO) = 8.1 \times 10^{-4}$) on the molality scale.

3.4. *Discussion*

Since the equilibrium potential of the zinc electrode obeys the Nernst equation, it may be assumed that the activity coefficient of zinc ions remains constant in molten LiCl–KCl eutectic containing high oxide molar fraction (10^{-4} and 10^{-3}) when the Zn(II) species mole fraction is below 1×10^{-3} and 3×10^{-2}, respectively. This agrees with a previously published study [1].

Although the purpose of this work was not to determine the value of the apparent standard potential of the couple Zn/Zn(II) in molten LiCl–KCl, values of $E^0_{Zn/Zn(II)}$ can be deduced from the experimental results. The order of magnitude obtained in the present study is consistent with values published in other literature: −756 mV/Ag–AgCl [1] and −729 mV/Ag–AgCl [19]. These authors suggested strong complexation of the Zn(II) species in such media [19–23].

Values of solubility product of zinc oxide at 450° C have already been published by other workers. The published values, calculated using the molality scale, are 2.1×10^{-2} in $ZnCl_2$–2NaCl [2] and 7.13×10^{-3} in LiCl–KCl eutectic containing 5 mol% $ZnCl_2$ [1]. The difference of two orders of magnitude between our result (8.1×10^{-4}) and that obtained in $ZnCl_2$–2NaCl [2] can be explained by the different acidities of the two media. In LiCl–KCl eutectic containing 5 mol% $ZnCl_2$, the difference of one order of magnitude may result from the method of determination based on the complete dissociation of sodium carbonate [1], which may fail as shown above. Nevertheless, the value deduced in LiCl–KCl eutectic is satisfactory, considering the two consistent results obtained from different tests and the comparison with published data.

4. Conclusion

This work confirms the use of the zirconia electrode in molten LiCl–KCl at 450° C to measure the oxoacidity of this medium and showed the sensitivity of the electrode potential response to changes in oxide concentration. The electrode calibration was successful for values of pO^{2-} ranging from 2 to 13 and showed the necessity of using the 'weighed additions' method carefully. The method is widely employed because it is simple experimentally and theoretically but problems result due to the kinetics of the carbonate decomposition reaction. Calibration of the electrode, based on an oxoacido-basic buffer system, is the best method.

The study of the zinc oxoacidity properties in molten LiCl–KCl eutectic at 450° C consisted in the determination of the solubility product of zinc oxide ZnO. The determination of K_S by titrating a Zn(II) solution by oxide ions was disturbed by the slow kinetics of carbonate decomposition. Therefore the solubility product was obtained by precipitating ZnO oxide by anodic oxidation of Zn(II) species into molten LiCl–KCl eutectic containing an oxide concentration fixed by the CO_3^{2-}/CO_2 buffer system. From the evolution of the zinc electrode potential with respect to the Zn(II) species concentration, values of $K_S(ZnO)$ and $E^0_{Zn/Zn(II)}$ were obtained and were consistent with other published data.

References

[1] M. Jafarian, 'Contribution à l'étude du raffinage électrochimique du zinc en milieu de chlorures fondus', Thesis-INP Grenoble (1990).
[2] D. Ferry, Y. Castrillejo and G. Picard, *Electrochim. Acta* **34** (1989) 313.
[3] R. Combes, J. Vedel and B. Tremillon, *ibid.* **20** (1975) 191.
[4] D. Flinn and K. H. Stern, *J. Electroanal. Chem.* **63** (1975) 39.
[5] J. P. Schnell, Thesis, Paris (1977).
[6] R. Lisy and R. Combes, *J. Electroanal. Chem.* **83** (1977) 287.
[7] R. Combes, B. Tremillon and F. de Andrade, *ibid.* **83** (1977) 297.
[8] R. Combes, R. Feys and B. Tremillon, *ibid.* **83** (1977) 383.
[9] R. Combes, M. N. Levelut and B. Tremillon, *ibid.* **91** (1978) 125.
[10] G. Picard, F. Seon and B. Tremillon, *ibid.* **102** (1979) 65.
[11] M. Jafarian and J. Bouteillon, *Electrochim. Acta* **35** (1990) 1201.
[12] J. Bouteillon and A. Marguier, *Surf. Technol.* **22** (1984) 205.
[13] B. Tremillon and G. Picard, Proc. 1st International Symposium on 'Molten Salt Chemistry and Technology', Molten Salt Committee, Electrochemical Society of Japan, Kyoto (1983) p. 33.
[14] D. Ferry, E. Noyon and G. Picard, *J. Less-common Metals* **97** (1984) 331.
[15] 'International Critical Tables', vol. 3, McGraw-Hill, New York/London (1928) pp. 54 and 301.
[16] R. Littlewood, *Electrochim. Acta* **3** (1961) 270.
[17] M. Hansen, 'Constitution of Binary Alloys', McGraw-Hill, New York (1958).
[18] R. Combes, J. Vedel and B. Tremillon, *J. Electroanal. Chem.* **27** (1970) 170.
[19] H. A. Laitinen and C. H. Liu, *J. Am. Chem. Soc.* **80** (1958) 1015.
[20] L. Yang and R. G. Hudson, *Trans. Met. Soc. AIME* **215** (1959) 589.
[21] G. Hevesy and E. Lowenstein, *Z. Anorg. und Allg. Chem.* **187** (1930) 266.
[22] J. C. Corbett, S. V, Winbush and F. C. Albers, *J. Am. Chem. Soc.* **79** (1957) 3020.
[23] Z. Gregorczyk, *Pr. Nauk. Inst. Chem.* **19** (1973) 99.